2020 Building Performance Analysis Conference and
SimBuild co-organized by ASHRAE and IBPSA-USA

ENERGY ANALYSIS OF STEAM DISTRIBUTION SYSTEM USING A PHYSICS-BASED MODEL: A CAMPUS BUILDING CASE STUDY

Behzad Salimian Rizi[1], Akram Syed Ali[1], Christopher Riley[1], Brent Stephens[1], Mohammad Heidarinejad[1]

[1] Illinois Institute of Technology, Chicago, IL, 60616, USA

ABSTRACT

This study develops a physics-based model to assess the performance of a hydronic steam radiator heating system and steam consumption in a historic campus building located in Chicago, IL. The physics-based model considered all components of the radiator heating system in the building, including distribution pipes, radiators, district steam, valves and fittings and applied mass and energy balance equations to (i) investigate the variation of pressure and temperature in the steam distribution network (SDN) and (ii) determine the steam mass flow rate at the building level according to the zone-level steam velocity. The model was calibrated with the amount of measured pressure and temperature at the building level. Model results provide insight into the likely behavior of the steam distribution system under different conditions. For example, changing the steam velocity at the zone-level from 10 m/s to 30 m/s results in a 7-fold increase in the pressure drop between the furthest node of the SDN and the building level. Moreover, the estimated temperature loss between the first node and the furthest node of the SDN (node 22) is 14.5 °C. The model approach enables detailed energy audits for informing energy efficiency measures for steam distribution systems.

INTRODUCTION

Applications of district heating systems in the U.S. originate back to as early as the 18th century. Nowadays a significant number of institutions in the U.S. benefit from district heating and cooling systems [1]. District heating systems, including steam and high temperature hot water systems, are among the main heating distribution systems for campuses. Hot water temperature systems have various advantages over steam distribution systems since they operate at lower temperature. Additional advantages include flexibility of piping distribution systems, lower maintenance costs, better safety, and better temperature control [2]. Thus, there are interests to replace steam district heating systems with hot water systems [3]. Overall, these systems usually operate using fossil fuels in the U.S., which contributes to greenhouse gas (GHG) emissions. Consequently, an accurate understanding and prediction of energy consumption are important to assess potential saving measures and develop effective energy management strategies.

Since the main parts of a steam district heating system are boilers and distribution systems, it is crucial to apply different energy efficiency measures (EEMs). The measures related to boilers include process control, excess air, insulation, flue gas quantities, heat recovering and boiler maintenance. Measures related to distribution system is comprised of insulation, steam traps, leaks and recovering. Currently, based on prior experience in campus energy efficiency management, these measures, as well as utility incentives for these measures, are commonly installed in an ad hoc approach. To bridge this knowledge gap, this study aims to provide a modeling approach that can evaluate impacts of different EEMs related to district heating systems [4].

To emphasize the importance of hydronic systems, this study utilizes the Commercial Building Energy Consumption Survey (CBECS) dataset to investigate two main heating systems including boiler inside the building (BLR) and district steam or hot water (DH) [5]. BLR and DH are classified in hydronic system category and each of them categorized into seven different systems. Since this study focuses on analyzing the heating systems connected to radiators, two selected CBECS categories are (1) boiler system connected to radiator (BLRRAD) and and (2) district hot water/steam connected to radiator (DHRAD). To compare the radiator distributions, five other systems are considered in addition to BLRRAD and DHRAD. It should be mentioned the CBECS data showed buildings used a combination of hydronic systems. Figure 1 and Figure 2 investigate the distribution of various types of the boiler system and district heat system before 1990 in different census of the U.S., respectively. As Figure 1 and Figure 2 show, about 65% of buildings located in the Northeast, East North Central, West North Central and North West are built before 1990 and use BLRRAD

and DHRAD systems.

There are various studies on the use of radiator systems in district heating systems in commercial and residential buildings. One study created the simulation model for the whole building including detailed dynamic components of the heating system to quantify the distribution and emission losses of a radiator heating system [6]. The results show that thermostats using a Proportional Integral (PI) controller play an important role for distribution losses with low temperature heating curves and emission losses. Control losses created by proportional thermostats are between 2% and 6%. A recent study provides statistics on the radiator temperature located in Gothenburg's for 109 rooms and quantified the supply and return temperatures for different design outdoor temperatures [7]. Another study developed a physics-based model to analyze heat drop and exergy loss of a steam power plant and all its equipment. The results demonstrated that condenser dissipates about 69.8% of the total dissipated energy, which is considered as the significant part of lost energy in the cycle [8]. However, the physics-based studies do not provide opportunities to learn from the historical data to easily predict future conditions. However, none of these studies have looked at detailed impacts of various parameters in a district heating system. This study aims to develop a physics-based model that considers both the zone level details (i.e., uncertainties introduced by occupants) and the building level details to monitor the variation of temperature and pressure at different nodes of the SDN.

METHODS

This study develops a physics-based model based on mass and energy conversation equations to calculate mass flow rate, velocity, pressure, temperature and specific volume at different nodes of the SDN. Energy Equation Solver (EES) is applied for performing analysis [9]. The SDN includes pipes, steam risers, district steam, gate valves, T-branches, elbows, and contraction joints at the south and east side of the building. The model starts from the basement (after the building's main pressure reduced valve (PRV)) and terminate at the radiator's inlet. The exact location of the steam risers and fittings, pipe length and diameter are determined from the mechanical drawings of the building. There are 10 steam risers at the south and east sides, and they are connected to two radiators each. Figure 3 shows the schematic of the SDN on the south and east sides of the building. The characteristics of the SDN are presented in Table 1.

The high-pressure steam after passing through the PRV valve at the basement enters to the SDN at 48.25 kPa and 115 °C. The pressure gage and temperature sensor at the basement are shown in Figure 4.

Table 1. Length of pipe sections in the SDN

Pipe section	Length (m)
1-2-3-4	25
1-2-5-6	17
1-2-7-8	19
1-2-9-10	27
1-2-11-12	34
1-2-13-14	41
1-2-15-16	48
1-2-17-18	56
1-2-19-20	66
1-2-21-22	79

Six steps conducted in this study for the modeling steps and the set of equations are as follow:

- Step 1: Assign velocity at the end of the steam risers based on volumetric flow rates.
- Step 2: Determine steam specific volume according to pressure and temperature at different nodes.
- Step 3: Determine the temperature at different nodes of steam distribution network.
- Step 4: Determine the pressure at different nodes of steam distribution network.
- Step 5: Assign the initial value for the pressure at the end of steam riser.
- Step 6: Validate the model with measured data.

Step 1: Steam velocity at the zone-level is a key input for the physics-base analysis since it indicates the volumetric flow rate ($\dot{Q}_i$) at the inlet of radiators. This study considers 10 m/s and 30 m/s as a steam velocity at the end of steam risers [10].

Step 2: Specific volume of steam at each node is an important feature in determining the mass flow rate. Specifc volume is a thermodynamic peroperty which is a function of temperature and pressure as shown in Equation (1).

$$v_i = f(steam, \mathrm{T_i}, \mathrm{P_i}) \quad (1)$$

Step 3: Temperature at different nodes of the SDN is needed due to the heat losses through the pipes and fittings. In order to consider the effect of heat losses and monitor the temperature changes throughout the SDN, Equation (2) is used.

$$T_{i-1} = T_i(1 + \alpha) \quad (2)$$

where $\mathrm{T_i}$ demonstrates temperature at node i, and T_{i-1} is the temperaturte at node i located upstream. α is a varible

whose value depends on temperature boundary conditions, length of the pipe, and location of nodes in the distribution network. Temperature sensor at node 22 (Figure 3) shows a temperature reading of 101 ℃. α parameter is defined between 0 and 0.01 ($0 \leq \alpha \leq 0.01$) according to the temperature at node 1 and 22 and length of the pipe sections given in Table 1. α is considered as 0.01 for all the steam risers, and for the nodes located at the inlet and outlet of each fitting, including 90° bend or T- branches, the temperature differences are assumed to be zero (α=0). The unit of temperature in Equation (2) is degree Fahrenheit. The set of equations which is applied for determining the temperature at different nodes is as follows:

$$\begin{aligned}
T_j &= T_{22} + \Delta T_{22-j} = T_{20} + \Delta T_{20-j} \\
T_h &= T_j + \Delta T_{j-h} = T_{18} + \Delta T_{18-h} \\
T_g &= T_h + \Delta T_{h-g} = T_{16} + \Delta T_{16-g} \\
T_f &= T_g + \Delta T_{g-f} = T_{14} + \Delta T_{14-f} \\
T_e &= T_f + \Delta T_{f-e} = T_{12} + \Delta T_{12-e} \\
T_d &= T_e + \Delta T_{e-d} = T_{10} + \Delta T_{10-d} \\
T_c &= T_d + \Delta T_{d-c} = T_8 + \Delta T_{8-c} \\
T_b &= T_c + \Delta T_{c-b} = T_6 + \Delta T_{6-b} \\
T_a &= T_b + \Delta T_{b-a} = T_4 + \Delta T_{4-a} \\
T_1 &= T_a + \Delta T_{a-1}
\end{aligned} \tag{3}$$

By using Equation set (3), temperatures at nodes 2, 4, 6, 8, 10, 12, 14, 16, 18, 20 and 22 are determined. Figure 5 depicts the temperature at different nodes of the SDN.

Step 4: Pressure is another important factor for determining the steam mass flow rate. In order to determine the pressure at each node of the SDN, similar to the temperature calclulation, start from the end of the steam risers and back to the beginning of steam risers, main pipe and finally node 1 is applied for pressure with this difference that initial pressure (P_i) is assigned for (i=4, 6, 8, 10, 12, 14, 16, 18, 20 and 22). Since the pressure at node 1 is 48.25 kPa ($P_1 = 48.25\ kPa$), and pressure at node 22 become 34.5 kPa (by moving from node 1 to node 22 and velocity of 30 m/s), the assigned values for the pressure at each node is considered to be between 34.5 kPa and 48 kPa. For this purpose, a parametric table is used to change the pressure at every selected node (i.e., 4, 6, 8, 10, 12, 14, 16, 18, 20, 22) 0.5 kPa as shown in Equation (4).

$$P_{k+1,i} - P_{k,i} = 0.5 \qquad 1 \leq k \leq 28 \tag{4}$$

where k represents the row number in the parametric table and i represents the node number at SDN.
According to the assigned values for the pressure at node i (i=4, 6, 8, 10, 12, 14, 16, 18, 20 and 22) the pressure at other nodes are determined by Equation (5).

$$\mathrm{P_{i-1}} = \mathrm{P_i} + \Delta \mathrm{P_{i,i-1}} \tag{5}$$

where $\mathrm{P_i}$ demonstrates the pressure at node i and $\mathrm{P_{i-1}}$ is the pressure of node located upstream. $\Delta \mathrm{P_{i,i-1}}$ is calculated based on the Darcy–Welsbach equation as follows:

$$\Delta \mathrm{P_{i,i-1}} = K_i \ \frac{V_i^2}{2g} \tag{6}$$

where K_i and V_i represent the resistance coefficient and velocity at node i, respectively. K_i depends on the type of fitting. In this model, $K_{90° Elbow}$, $K_{T-branch}$, $K_{T-straight}$, $K_{Contraction}$, $K_{Gatevalve}$, and K_{pipe} are applied based on the mechanical drawings of the building. The pressure loss through the gate valve is highly dependent on fraction opening (FO) of the gate valve ($0 \leq FO \leq 1$) [11]. The velocity at each node is determined by Equation (7):

$$\mathrm{V_i} = v_i \dot{\mathrm{m}}_\mathrm{i} / \mathrm{A_i} \tag{7}$$

Mass flow rate ($\dot{\mathrm{m}}_\mathrm{i}$) is determined by Equation (8) for the nodes located at the radiator inlet

$$\dot{\mathrm{m}}_\mathrm{i} = \frac{V_i \mathrm{A_i}}{v_i} \ (\mathrm{i} = 4, 6, 8, 10, 12, 14, 16, 18, 20, 22) \tag{8}$$

where v_i is derived by an iterative process using Equation (1). Also, $\mathrm{V_i}$ for (i=4, 6, 8, 10, 12, 14, 16, 18, 20 and 22) is determined by step 1. For the ones located in the main pipe, mass balance equation is applied as Equation (11) shows:

$$\begin{aligned}
\dot{m}_j &= \dot{m}_{19} + \dot{m}_{21} & \dot{m}_h &= \dot{m}_j + \dot{m}_{17} \\
\dot{m}_g &= \dot{m}_h + \dot{m}_{15} & \dot{m}_f &= \dot{m}_g + \dot{m}_{13} \\
\dot{m}_e &= \dot{m}_f + \dot{m}_{11} & \dot{m}_d &= \dot{m}_e + \dot{m}_9 \\
\dot{m}_c &= \dot{m}_d + \dot{m}_7 & \dot{m}_b &= \dot{m}_c + \dot{m}_5 \\
\dot{m}_a &= \dot{m}_b + \dot{m}_4
\end{aligned} \tag{9}$$

where $\dot{m}_a$ indicates the steam mass flow rate at the south side of the building.

Step 5: In this part, an initial guess for the pressure at the furthest node of the SDN (P_{22}) is selected from the Equation 4. Pressure at node 20 is calculated according to the initial guess for P_{22} and Equation 10.

$$P_j = P_{22} + \Delta P_{22-j} = P_{20} + \Delta P_{20-j} \tag{10}$$

since the P_{20} is updated, v_{20}, mass flow rate at steam riser 9 and consequently velocity and mass flow rate at node j are updated as well as P_h. The same approach is implemented for the upstream nodes and steam risers as Equation (11) to identify the exact value for the pressure.

$$
\begin{aligned}
P_h &= P_j + \Delta P_{j-h} = P_{18} + \Delta P_{18-h} \\
P_g &= P_h + \Delta P_{h-g} = P_{16} + \Delta P_{16-g} \\
P_f &= P_g + \Delta P_{g-f} = P_{14} + \Delta P_{14-f} \\
P_e &= P_f + \Delta P_{f-e} = P_{12} + \Delta P_{12-e} \\
P_d &= P_e + \Delta P_{e-d} = P_{10} + \Delta P_{10-d} \\
P_c &= P_d + \Delta P_{d-c} = P_8 + \Delta P_{8-c} \\
P_b &= P_c + \Delta P_{c-b} = P_6 + \Delta P_{6-b} \\
P_a &= P_b + \Delta P_{b-a} = P_4 + \Delta P_{4-a}
\end{aligned} \tag{11}
$$

Step 6: In the last step, the calibration process for the created model is applied. The pressure at node 1 is determined by Equation (12) using the initial guess value for the pressure at node 22 (P_{22}) and is compared with the measured pressure ($P_{1-measured}$) using an existing sensor network in the building [12].

$$P_{1-model} = P_a + \Delta P_{a-1} \tag{12}$$

The pressure at node 1 from the measurement is 48.25 kPa. If the differences between $P_{1-model}$ and $P_{1-measured}$ are not negligible (i.e., more that 2% difference), the initial guess (P_{22}) should be changed in order to get a minimum difference between them.

RESULTS

In the following, based on the presented method for determining pressure, the pressure at different nodes of the SDN is calculated at velocities 10 m/s and 30 m/s and with a fraction opening of the gate valves of 0.5 and 1. $P_{1-measured}$ is 48.25 kPa for four different scenarios. By selecting initial guess for P_{22} and using Equations (10) and (11), $P_{1-model}$ is calculated from Equation (12). As shown in Table 2 and Table 3, the calculated $P_{1-model}$ (node 1) is close to the $P_{1-measured}$, which means that the model performs well according to this criterion. Table 2 and Table 3 present the pressure at different nodes of the SDN and demonstrate that velocity is one of the important factors for pressure head losses through the network. At an assumed velocity of 30 m/s, the steam pressure at the furthest node (node 22) from the PRV (node 1) is 6 kPa lower than the pressure at the same node at an assumed velocity of 10 m/s. Also, FO of the gate valves is one of the significant parameters at higher velocities. The pressure differences at the same node at higher velocities is much greater than those at lower velocities. At a velocity 30 m/s, the pressure difference at the same node in fully opened valve position is about 1 to 1.5 kPa is greater than half opened, while at velocity 10 m/s, the pressure differences are negligible.

For better understanding, Figure 6 shows the results in bar graphs. In the last step, the calculated values for temperature and pressure at different nodes of the SDN and Equations 4 to 14 are used to calculate the steam mass flow rate at the building level. Steam mass flow rate at velocity of 10 m/s and 30 m/s are 0.017 kg/s and 0.051 kg/s, respectively. It means that the steam velocity plays an important role in determining the steam mass flow rate.

Table 2. Pressure value (kPa) at different nodes of the SDN applying 2 scenarios for V=10 m/s

Node	FO = 0.5	FO = 1	Node	FO = 0.5	FO = 1
1	48.33	48.30	4	48.11	48.20
6	47.85	48.00	a	48.26	48.30
8	47.82	47.97	j	47.46	47.60
10	47.70	47.86	h	47.67	47.80
12	47.64	47.78	g	47.70	47.90
14	47.61	47.78	f	47.73	47.90
16	47.55	47.72	e	47.77	47.90
18	47.54	47.70	d	47.84	48.00
20	47.31	47.47	c	47.94	48.10
22	47.23	47.38	b	47.97	48.10

Table 3. Pressure value (kPa) at different nodes of the SDN applying 2 scenarios for V=30 m/s

Node	FO = 0.5	FO = 1	Node	FO = 0.5	FO = 1
1	48.81	48.66	4	47.26	47.40
6	44.92	46.25	a	48.58	48.40
8	44.74	46.06	j	42.23	43.50
10	44.02	45.33	h	43.78	45.10
12	43.51	44.78	g	43.97	45.30
14	43.16	44.45	f	44.16	45.50
16	42.98	44.26	e	44.50	45.80
18	42.82	44.06	d	45.03	46.40
20	41.18	42.40	c	45.77	47.10
22	40.61	41.81	b	45.95	47.30

CONCLUSION

This study presents a new integrated zone-to-building level modeling approach to assess the operation of a steam distribution system in a historic campus building located in Chicago, IL. The model develops a relationship between the zone-level steam velocity and steam mass flow rate at the building level using mass and energy balance equations. The model utilizes different steam velocities at the inlet of the radiators to investigate the variation of pressure and temperature at different nodes of a steam distribution network (SDN). Ultimately, this study calculates the steam mass flow rate at the building level.

The derived temperature at different nodes of SDN demonstrates that due to heat losses through the network, the maximum temperature difference between node 1 and the furthest node of the SDN (node 22) is about 14.5 °C. Results showed that by changing the zone-level steam velocity from 10 m/s to 30 m/s, the steam consumption at the building level becomes three times higher, while the pressure at the furthest node of the SDN changes from 47.4 kPa to 41.8 kPa (i.e., the pressure drop between the furthest node of SDN and building level becomes 7 times higher) when considering a constant pressure at the SDN inlet. In order to calibrate the model, derived pressure at the inlet of SDN from physics-based model was compared with measured data and finally the model was calibrated in a good agreement (i.e., 98% accuracy) between measured and physics-based model results. This new modeling approach has implications for (i) large numbers of buildings based on the conducted CBECS analyses (i.e., about 65% of buildings located in Northeast, East North Central, West North Central and North West are built before 1990 use radiator systems) and (ii) building energy simulations where the uncertainties introduced by occupants is considered as an important factor.

ACKNOWLEDGEMENT

This work was funded by an ASHRAE New Investigator Award to Mohammad Heidarinejad and Franklin Energy.

NOMENCLATURE

Variable	Description
A	Cross-section area (m^2)
FO	Fraction Opening
g	Gravitational acceleration (m/s^2)
K	Resistance Coefficient
$\dot{m}$	Mass flow rate (kg/s)
P	Pressure (kPa)
$\dot{Q}$	Volumetric flow rate (m^3/s)
ν	Specific volume (m^3/kg)
Vol	Volume (m^3)
V	Velocity (m/s)
t	Time (s)
T	Temperature (℃)

REFERENCES

[1] Heidarinejad, M., Cedeno-Laurent, J. G., Wentz, J. R., Rekstad, N. M., Spengler, J. D., Srebric, J. 2017. Actual building energy use patterns and their implications for predictive modeling, Energy Conversion and Management 144, 2017, 164-180. https://doi.org/10.1016/j.enconman.2017.04.003

[2] Oliker, I. How Modern Hot Water Systems Can Lower Campus Energy. HPAC Engineering. https://www.hpac.com/heating/article/20929899/how-modern-hot-water-systems-can-lower-campus-energy-use

[3] FVB Energy INC. Steam to Hot Water Conversion. http://www.fvbenergy.com/wp content/uploads/FVB-Energy-Steam-to-Hot-Water-Conversion Experience.pdf

[4] Einstein, D., Worrell, E., Khrushch, M., 2001. Steam Systems in Industry: Energy Use and Energy Efficiency Improvement Potentials, ACEEE's 2001 Summer Study on Energy Efficiency in Industry Proceedings.

[5] 2012 Commercial Building Energy Consumption Survey Data, https://www.eia.gov/consumption/commercial/data/2012/

[6] Maivel, M., Kurnitski, J. 2013. Low temperature radiator heating distribution and emission efficiency in residential buildings. Energy and Buildings 69, 2014, 224-236. https://doi.org/10.1016/j.enbuild.2013.10.030

[7] Jangsten, M., Kensby, J., Dalenbäck, J.-O., Trüschel, A. 2016. Survey of radiator temperatures in buildings supplied by district heating. Energy 137, 2017, 292-301. https://doi.org/10.1016/j.energy.2017.07.017.

[8] Ahmadi, G.R., Toghraie, D. 2016. Energy and exergy analysis of Montazeri Steam Power Plant in Iran, Renewable and Sustainable Energy Reviews 56, 2016, 454-463. https://doi.org/10.1016/j.rser.2015.11.074.

[9] F-Chart Software. 2019. Energy Equation Software (10.644 Academic Commercial)

[10] Dryden, I.G.C., 1982. The efficient use of energy. 2nd edition. ISBN: 9781483101576

[11] Engineering Department: Crane Co. 2010. Flow of fluids through valves, fittings and pipe. Technical Paper No. 410. ISBN 1-40052-712-0

[12] Syed Ali, A., Coté, C., Heidarinejad, M., Stephens, B. 2019. Elemental: An Open-Source Wireless Hardware and Software Platform for Building Energy and Indoor Environmental Monitoring and Control, Sensors 2019, 19, 4017. https://doi.org/10.3390/s19184017

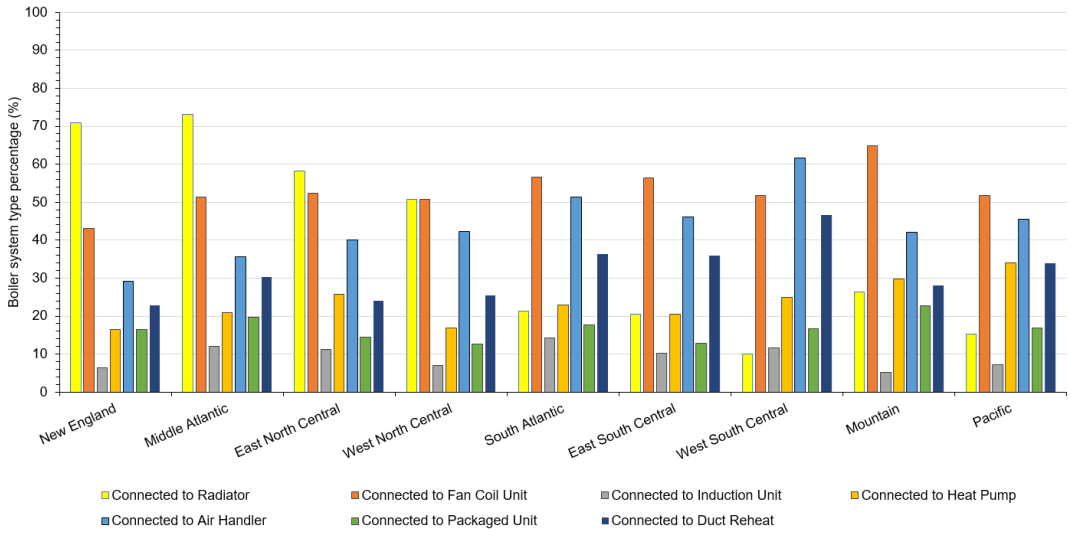

Figure 1. Percentage of pre-1990 buildings with boiler system types vs census division

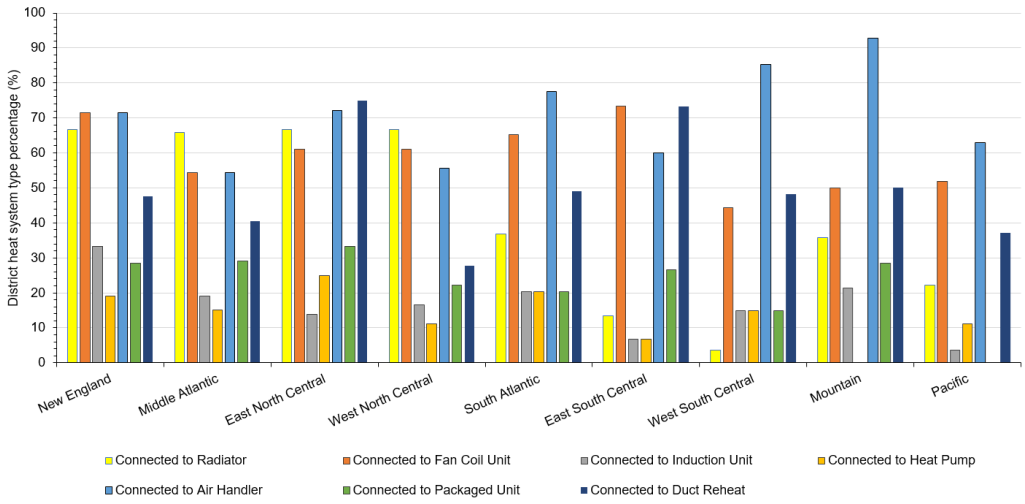

Figure 2. Percentage of pre-1980 buildings with district heating system types vs census division

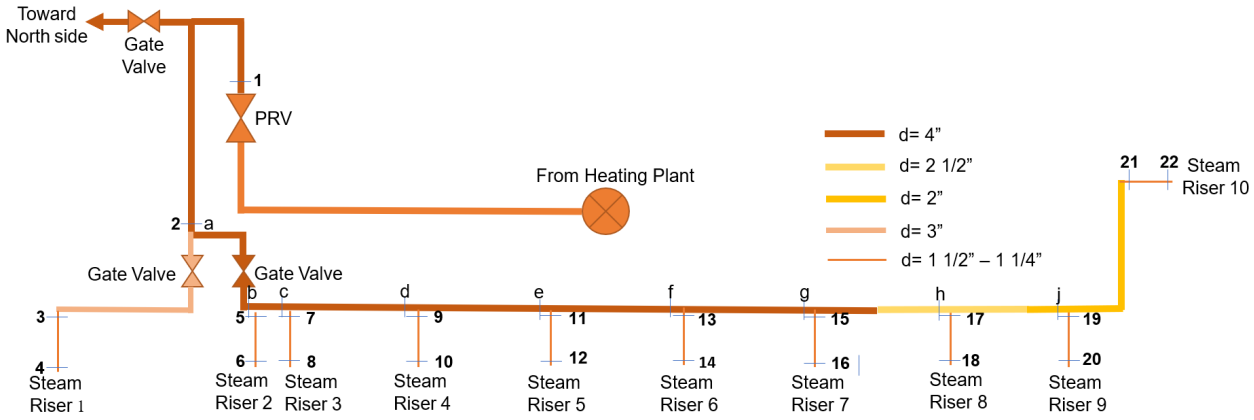

Figure 3. Schematic of the SDN at the south and east side of the building

(a) (b)

Figure 4. Temperature sensor and (b) Pressure gage installed after PRV

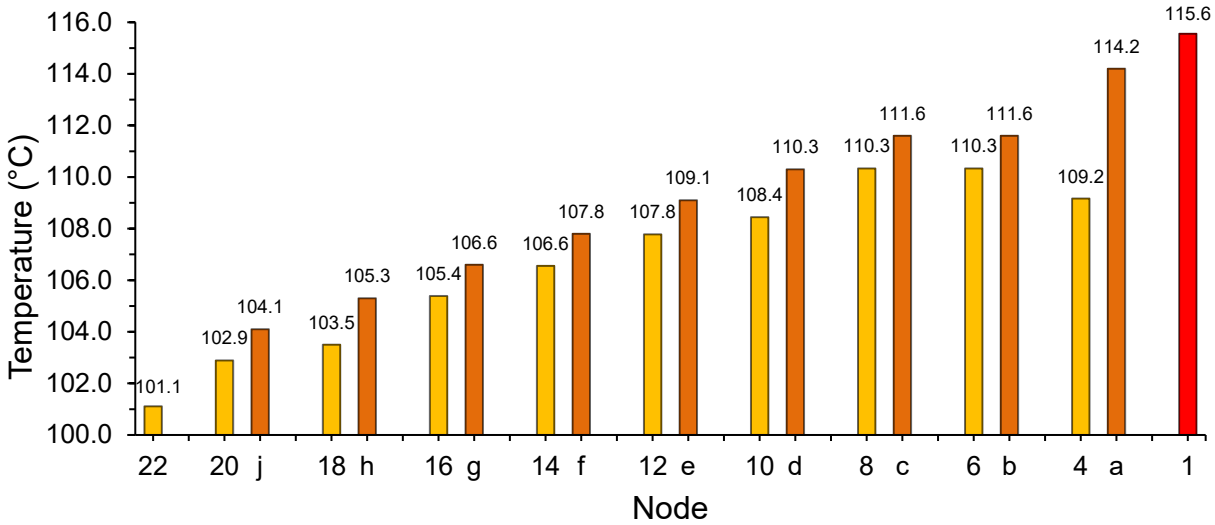

Figure 5 Temperature values at different nodes of the SDN

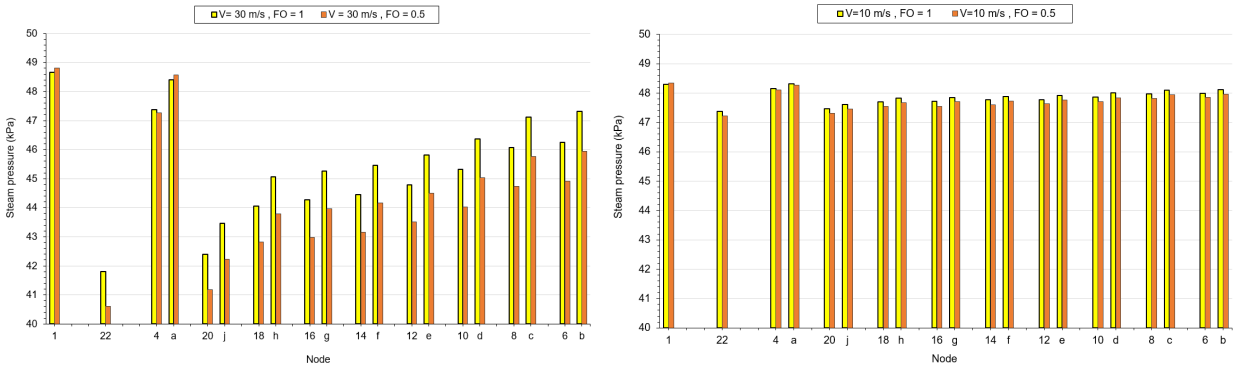

(a) *(b)*

Figure 6. Steam pressure for different nodes at (a)V=30 m/s, FO=0.5 and FO=1 and (b) V=10 m/s, FO=0.5 and FO=1